

The Mean Type Ia Supernova Spectrum Over the Past 9 Gigayears

M. Sullivan¹, R. S. Ellis^{1,2}, D. A. Howell^{3,4}, A. Riess⁵, P. E. Nugent⁶, A. Gal-Yam⁷

sullivan@astro.ox.ac.uk

ABSTRACT

We examine the possibility of evolution with redshift in the mean rest-frame ultraviolet (UV; $\lambda \lesssim 4500\text{\AA}$) spectrum of Type Ia Supernovae (SNe Ia) sampling the redshift range $0 < z < 1.3$. We find new evidence for a decrease with redshift in the strength of intermediate-mass element (IME) features, particularly Si II and to a lesser extent Ca II ‘H&K’ and Mg II blends, indicating lower IME abundances in the higher redshift SNe. A larger fraction of luminous, wider light-curve width (higher “stretch”) SNe Ia are expected at higher redshift than locally, so we compare our observed spectral evolution with that predicted by a redshift-evolving stretch distribution (Howell et al. 2007) coupled with a stretch-dependent SN Ia spectrum. We show that the sense of the spectral evolution can be reproduced by this simple model, though the highest redshift events seem additionally deficient in Si and Ca. We also examine the mean SN Ia UV-optical colors as a function of redshift, thought to be sensitive to variations in progenitor composition. We find that the expected stretch variations are sufficient to explain the differences, although improved data at $z \sim 0$ will enable more precise tests. Thus, to the extent possible with the available datasets, our results support the continued use of SNe Ia as standardized candles.

¹Department of Astrophysics, University of Oxford, Keble Road, Oxford OX1 3RH, UK

²Department of Astrophysics, California Institute of Technology, MS 105-24, Pasadena, CA 91125 USA

³Las Cumbres Observatory Global Telescope Network, 6740 Cortona Dr., Suite 102, Goleta, CA 93117

⁴Department of Physics, University of California, Santa Barbara, Broida Hall, Mail Code 9530, Santa Barbara, CA 93106-9530

⁵Department of Physics and Astronomy, Johns Hopkins University, 3400 N Charles St, Baltimore, MD 21218 USA

⁶Lawrence Berkeley National Laboratory, 1 Cyclotron Rd., Berkeley CA 94720, USA

⁷Astrophysics Group, Faculty of Physics, Weizmann Institute of Science, Rehovot 76100, Israel

Subject headings: supernovae: general — cosmological parameters — ultraviolet:
general

1. Introduction

Type Ia Supernovae (SNe Ia) have emerged as the most practical and immediate path for improving our understanding of dark energy. Techniques have been perfected for locating and studying hundreds of events over the redshift range $0 < z < 1.5$ where dark energy manifests itself, and ambitious new facilities are being planned that will take this progress to the next level of precision. However, it remains the case that the use of SNe Ia as cosmological probes is purely empirical, exploiting relationships between photometric properties such as peak luminosity, color and light curve width, that result in distance estimates precise to $\simeq 7\%$ (Guy et al. 2007; Jha et al. 2007; Conley et al. 2008).

Early work by Hamuy et al. (1995, 1996) demonstrated that some of these photometric properties depend on their host galaxy type, with SNe Ia in spirals possessing wider light curves (higher “stretch”) and are more luminous than those in older elliptical hosts. This has subsequently been categorized in terms of (perhaps distinct) populations of ‘prompt’ and ‘delayed’ SNe Ia (Mannucci et al. 2005, 2006; Scannapieco & Bildsten 2005), whose properties appear to be governed by the star formation activity of the host galaxy and therefore age of the progenitor stellar population (Howell 2001; Sullivan et al. 2006). With star formation increasing at higher redshift, these demographic variations produce a shift to more luminous, wider light curve events with redshift (Howell et al. 2007). Sarkar et al. (2008) discuss the implications and possible biases introduced in dark energy studies.

A less well-understood variation is the scatter in the rest-frame SN Ia ultraviolet (UV) spectra from one event to another. Although model predictions differ in detail (e.g. Höflich et al. 1998; Lentz et al. 2000; Sauer et al. 2008), the form of the UV spectrum short-ward of 4000\AA is believed to be sensitive to progenitor composition and explosion physics. Given the difficulty of studying this wavelength range in nearby events, the most comprehensive studies have been accomplished using UV data redshifted into the visible at $z \simeq 0.5$ (Ellis et al. 2008; Foley et al. 2008a). Ellis et al. (2008, hereafter E08) found significant scatter in the UV continuum below $\simeq 4000\text{\AA}$, at a level which exceeds that predicted assuming quite significant metallicity variations in the current models.

As both SN Ia progenitor age and metallicity likely evolve with redshift, it is natural to ask whether any spectral variations likewise appear redshift-dependent. Recent work by

Foley et al. (2008a, hereafter F08) has tentatively identified a decrease with redshift, at $\sim 2\text{-}\sigma$ significance, in the strength of blend of lines (Fe II, Fe III, Si II) near 4800\AA in maximum-light SN Ia spectra, which they attribute to Fe III 5129\AA . In this letter, we examine the rest-frame $\lambda \lesssim 4500\text{\AA}$ spectrum of SNe Ia over $0 < z < 1.3$ by combining data gathered using Keck at $z \simeq 0.5$ (E08) and Hubble Space Telescope (*HST*) at $z > 1$ (Riess et al. 2007, hereafter R07). Following Howell et al. (2007), our goal is to investigate whether any spectral variations are present that represent an evolutionary trend, and whether these can be explained by the observed shift to more luminous events at higher redshifts.

2. SN Ia Spectral Samples

We compile spectra from three sources corresponding to high, intermediate and low redshift (z). The intermediate- z spectra are described in E08 together with all aspects of their reduction. Targets were drawn exclusively from the Supernova Legacy Survey (SNLS; Astier et al. 2006), forming a homogeneous sample representative of the SNLS parent sample. Host galaxy contamination is removed using photometry of the hosts, with the flux calibration corrected using contemporaneous imaging of the SN light curves. This galaxy subtraction is a critical step when examining ground-based spectra of high-redshift SNe, and an incorrect continuum subtraction can systematically affect line feature strengths and bias conclusions drawn from them; the wide wavelength range of SNLS data allow an accurate host removal on individual spectra. We degrade the spectra to a resolution of 20\AA in the rest-frame to match that of the high- z *HST* spectra discussed below (the typical width of SN Ia spectral features is $\gtrsim 100\text{\AA}$, or $\gtrsim 5$ resolution elements).

The $z > 0.9$ spectra are taken from the *HST* ACS grism campaigns of Riess et al. (2004) and R07. Host galaxy subtraction is less problematic as the SNe were resolved from their host due to the superior resolution of *HST*. Any host that may lie underneath the SN is subtracted by defining narrow “sky” regions above and below the SN trace and interpolating to derive the contamination. The resolution of the grism ($R = \lambda/\Delta\lambda \sim 200$ at 8000\AA) equates to $\sim 20\text{\AA}$ in the rest-frame at 4000\AA for a $z=1$ SN, improving for higher- z events. We rebin all spectra to the 20\AA wavelength scale.

At low- z , samples are heterogeneous in nature. Both the R07 and E08 samples were found with “rolling searches” and can be considered complete with regard to host galaxy and environment; the same is not true for local searches which frequently involve targeting known galaxies. We replace the sample used in E08 with that of Matheson et al. (2008, hereafter M08), which has the benefit of a homogeneous reduction technique, resulting in spectra that are close to spectrophotometric (M08). For each SN we select the closest spectrum to a

phase of +3d (the mean of the higher- z samples). Due to the large apparent size of the host galaxies, the surface brightness at the SN position is small. The M08 spectra are optical only, so at $\lambda \lesssim 3600\text{\AA}$, we supplement the sample with the space-based UV spectra of SN1992A (Kirshner et al. 1993), SN1981B (Branch et al. 1983) and SN2001ba (e.g. Foley et al. 2008b), the only three spectroscopically normal SNe Ia in the appropriate phase range.

The light curves of all the SNe Ia are fit using the SiFTO light curve fitter (Conley et al. 2008) to place their photometric parameters on the same system. The distributions in light curve phase (τ_{eff} ; measured in days relative to maximum light in the rest-frame B band divided by light curve stretch), z , stretch (s) and rest-frame $B - V$ color (\mathcal{C}), are shown in Figure 1. The high- z *HST* spectra are typically at a later phase due to the scheduling and search strategy used. Note that the SNLS, a rolling search, produces more early SN Ia spectra than more traditional search methods used at low- z . We restrict our analysis to a comparison sample of spectra with $-1 < \tau_{\text{eff}} < 8$ (important given the evolution in SN spectra with light curve phase), a stretch range of $0.8 < s < 1.30$, and a color range of $-0.2 < \mathcal{C} < 0.35$. We only consider “spectroscopically normal” SNe, excluding obvious, low-Si SN1991T-like events (Filippenko et al. 1992). The mean properties are given in Table 1.

The stretch distributions are marginally different, with evidence for an increase in mean stretch with redshift at $\sim 1.5\sigma$ significance, as expected following the analysis of Howell et al. (2007). The \mathcal{C} distributions of all three samples are consistent, arguing *against* the stretch differences arising primarily from selection effects related to search biases, as these would also be manifest in the color histograms. The sample of low- z SNe with UV spectra has a particularly low mean stretch, with two of these SNe at the lower end of the stretch range (SN1992a at 0.82 and SN1981b at 0.89).

Table 1. Mean properties of the SN Ia samples

\bar{z}	N	$\bar{\tau}_{\text{eff}}$	\bar{s}	$\bar{\mathcal{C}}$
1.16 (0.97 to 1.39)	12	3.5	1.087(23)	0.007(18)
0.48 (0.12 to 0.73)	18	2.0	1.042(20)	0.000(20)
0.02 (0.00 to 0.04)	18	2.8	0.993(25)	0.042(28)
0.01 (UV spectra only)	3	4.1	0.91(06)	-0.01(0.05)

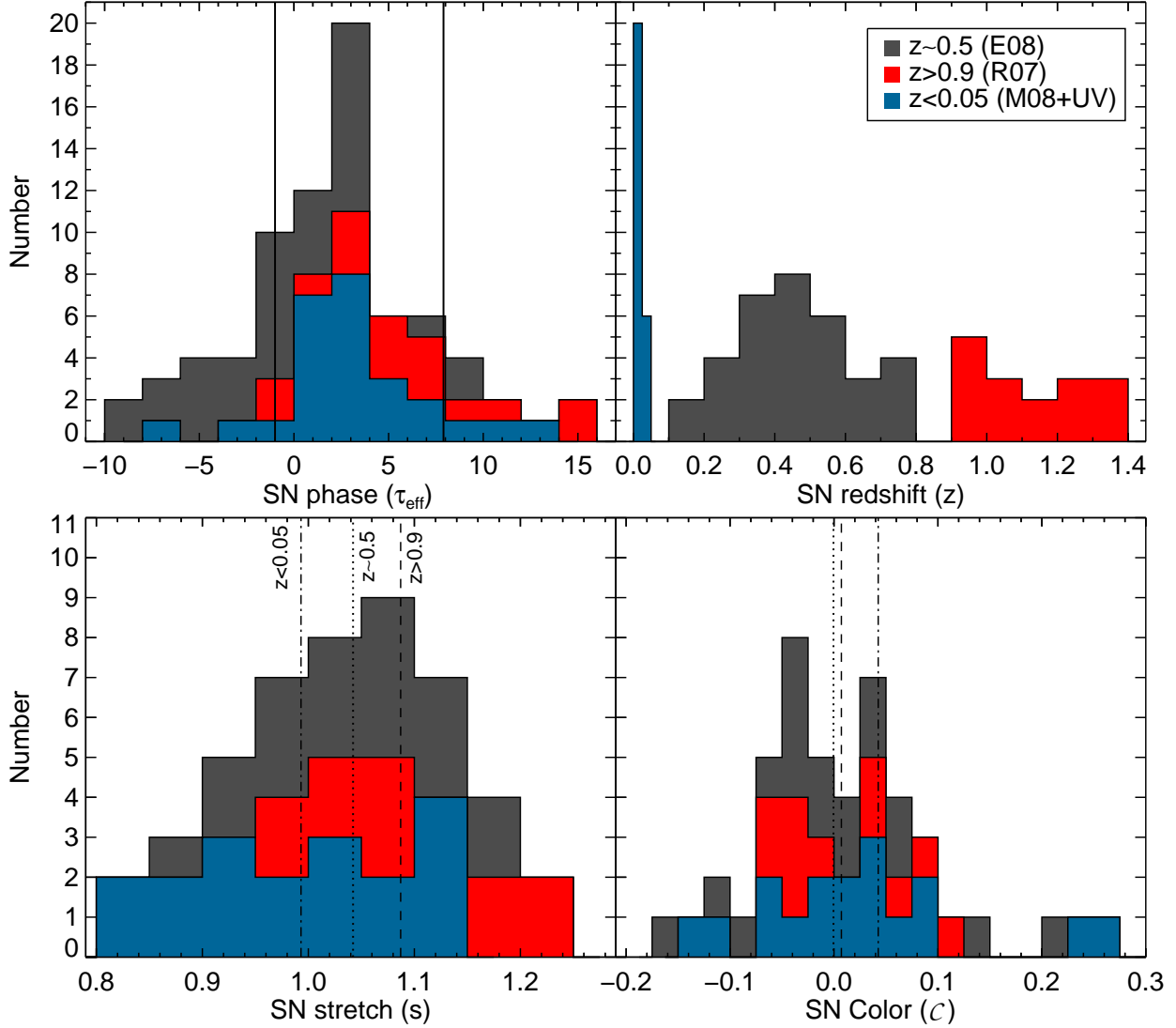


Fig. 1.— The distribution of various properties of the spectral sample. Upper left: The phase distribution of the entire sample. The vertical lines show the limits used to define the comparison samples. Upper right: The redshift distribution of the entire sample. Lower left: The SN stretch distribution for just the comparison sample. The dotted/dashed/dot-dash vertical lines show the weighted means for the SNLS/low- z /HST samples. Lower right: The SN color distributions, weighted mean colors marked.

3. Spectral Comparisons

We construct mean spectra for the three samples following E08. All spectra are corrected for Milky Way extinction and color-corrected using the SALT-2 color law (Guy et al. 2007), reducing, though not eliminating, dispersion among SN Ia spectra and aligning them in the mean (E08). The spectra are normalized to have the same flux through a box filter defined from rest-frame 3750 to 4100Å (denoted U'), chosen as a common wavelength region for all spectra (changing this wavelength range does not change our results). The error on the mean spectrum is estimated using a bootstrap resampling technique (see E08, for more details). R07 previously presented a mean spectrum for the high- z *HST* spectra (used in comparisons with lower-redshift by F08), calculated over a wider phase range with different error estimation techniques, and lacking color-corrections on the individual spectra. A comparison of this R07 mean with (e.g.) the intermediate- z mean of E08 would not be appropriate, so we rederive the *HST* mean for comparison on a consistent basis¹.

The comparison of the mean spectra is shown in Figure 2. As noted by previous authors conducting similar analyses, the spectra appear very similar. In particular, with the exception of the low- z UV mean spectrum, the agreement in the shape of the continua is remarkable, suggesting the color corrections made to the spectra based on their optical color are effective in aligning the spectra across the entire wavelength and z range. However, we find new evidence for variations in some ion feature strengths, most obviously around 4000Å at the position of the blueshifted Si II 4128Å feature. Since the luminosity of the SN Ia is controlled by the amount of ⁵⁶Ni synthesized in the explosion, for a Chandrasekhar-mass explosion, brighter explosions imply increased ⁵⁶Ni production at the expense of intermediate mass elements (IMEs)² such as Si, Ca and Mg. So to first order one would expect to see fewer IMEs in more luminous, or broader-lightcurve SNe. Indeed, the Si II 4128 feature has been shown to have a lower equivalent width in broader-lightcurve SNe Ia (Guy et al. 2007; Ellis et al. 2008) and, by extension, in SNe Ia originating in spiral galaxies (Bronder et al. 2008). Given the observed drift in mean stretch with z of the SN Ia population (Howell et al. 2007), arising from shifting demographics of the SN Ia population, a generic prediction of two-component prompt+delayed SN Ia rate models is that the amount of IMEs in general, and Si in particular, in the average high- z spectrum should be smaller (Howell et al. 2007). This is in the same sense as the trends observed in the comparison of the means in Figure 2.

¹The R07 SNe used are: HST05Str, HST05Gab, HST05Lan, HST04Pat, HST04Gre, HST04Eag, HST04Sas, SN2003az(Tor), SN2002fw(Aph), SN2003dy(Bor), HST04Omb, sn2002dd.

²Stable, nuclear statistical equilibrium elements like ⁵⁴Fe or ⁵⁸Ni play a role, but they are relatively constant from SN to SN (e.g. Mazzali et al. 2007), and have only a small effect on this argument.

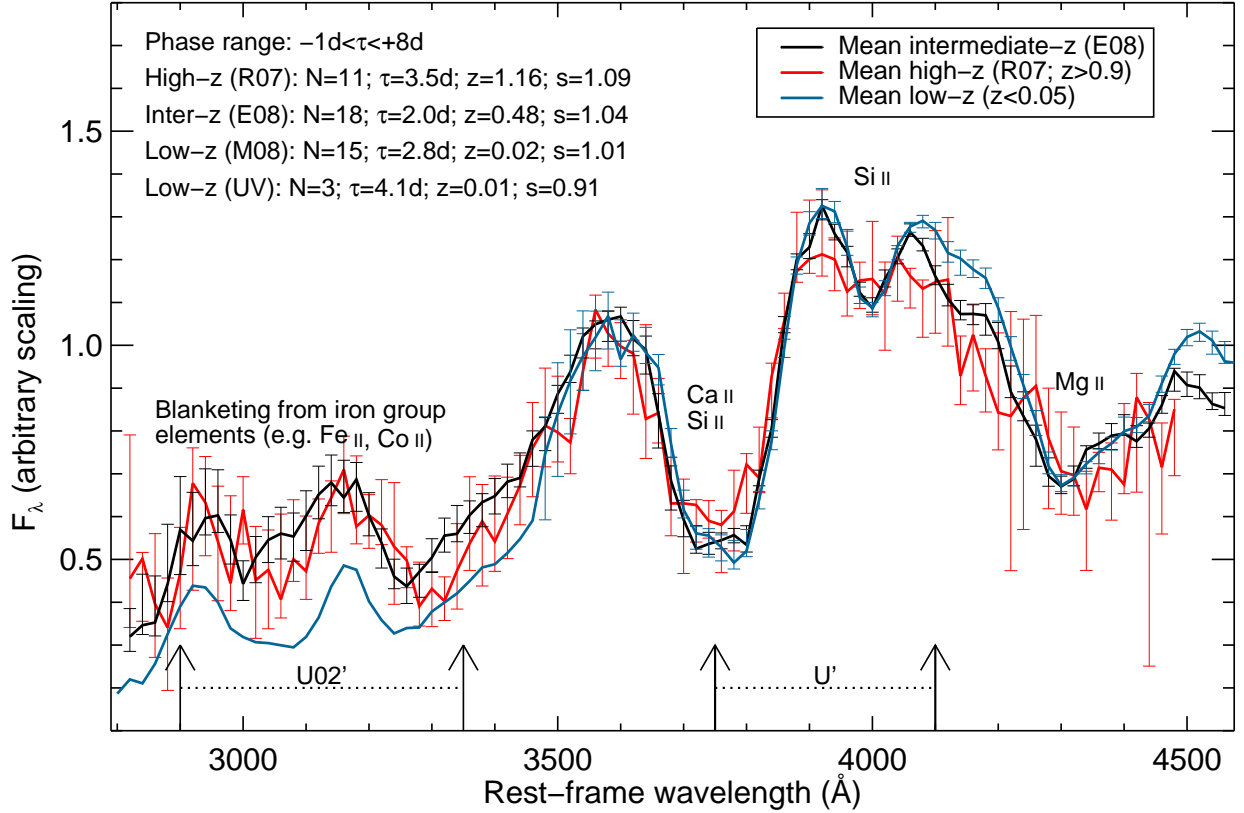


Fig. 2.— The comparison of the Keck-SNLS (black), low- z (blue) and *HST* (red) mean SN Ia spectra. The resolution is 20\AA and no additional smoothing is performed. The error bars are derived using a bootstrap resampling technique (see Ellis et al. 2008, for details). At $\lambda \lesssim 3500\text{\AA}$ in the low- z SNe, no error bars are plotted as only three SNe enter the sample. The vertical arrows show the boundaries of the U' (right) and $U02'$ (left) filters.

The interpretation of SN Ia spectra is complicated, and this simple picture may not tell the whole story. Observing a spectral feature in absorption only constrains the amount of material in a given ionization state, along the line of sight, above the photosphere at the time of the spectrum. At maximum light, approximately 2/3 of the mass of the SN Ia remains hidden under the photosphere (e.g. Höflich et al. 1998). One can imagine a pathological situation in which more luminous SNe Ia have fewer IMEs above the photosphere, and more below, but this would be at odds with the basic physical principle that fusion in denser regions produces heavier elements, a generic property of SN Ia models. Instead, a more likely complication is that more luminous SNe are hotter, and thus more ionized. In this situation, in the hottest regions Si II may be ionized to Si III, resulting in lower Si II equivalent widths (EWs). Fortunately, this potential complication does not change the basic principle that lower EWs of singly ionized IMEs are expected in the spectra of more luminous SNe Ia.

F08, comparing $z=0$ and $z=0.2-0.8$ mean spectra, find a lower strength in the Fe II blend at 4800\AA in higher- z spectra. F08 state they are unable to distinguish evolving SN Ia demographics with evolution in the SN properties. At first sight, their trend appears consistent with the results of this paper: higher-stretch SNe Ia will be hotter, and thus Fe ionized to Fe III at the expense of Fe II. However, the 4800\AA feature is a complex one, a blend of Si II (5041\AA , 5055\AA), Fe II (4923\AA , 5018\AA , 5169\AA) and Fe III (5129\AA) (e.g. Hatano et al. 1999). In fact, F08 attribute the weakening strength of the red side of the feature to Fe III which would be inconsistent with the simple picture outlined above. Given the presence of the other Fe II and Si II lines in this 4800\AA feature, further detailed modeling work is required before a robust conclusion with regards to this feature can be reached.

We investigate the variations in more detail by measuring the strength of three accessible IME spectral features (the blend of Ca II at rest-frame $\sim 3950\text{\AA}$ and Si II at $\sim 3860\text{\AA}$, Si II at 4128\AA , and Mg II at 4481\AA). We fit a Gaussian on a linear pseudo-continuum background and calculate the (pseudo) EW (e.g. Garavini et al. 2007). The error is estimated by performing the EW fit on each of the bootstrap resampled spectra and taking the standard deviation of the resulting distribution. The variation with redshift of these features is shown in Figure 3; the trends are for a decreasing EW for all three ions with increasing redshift. We emphasize that these measurements are made on mean spectra; in many cases the individual high- z spectra show evidence of Si II (R07).

Further into the UV, the continuum level shows a redshift-dependent trend, with the spectra broadly consistent from $0.5 < z < 1$, but depressed at $z < 0.05$. Potentially this is an important result; however the different SN Ia samples possess different mean stretches, and the UV-optical color of the higher-stretch samples may be expected to appear bluer (e.g. Guy et al. 2007; Ellis et al. 2008). Furthermore the paucity of local data and the intrinsic

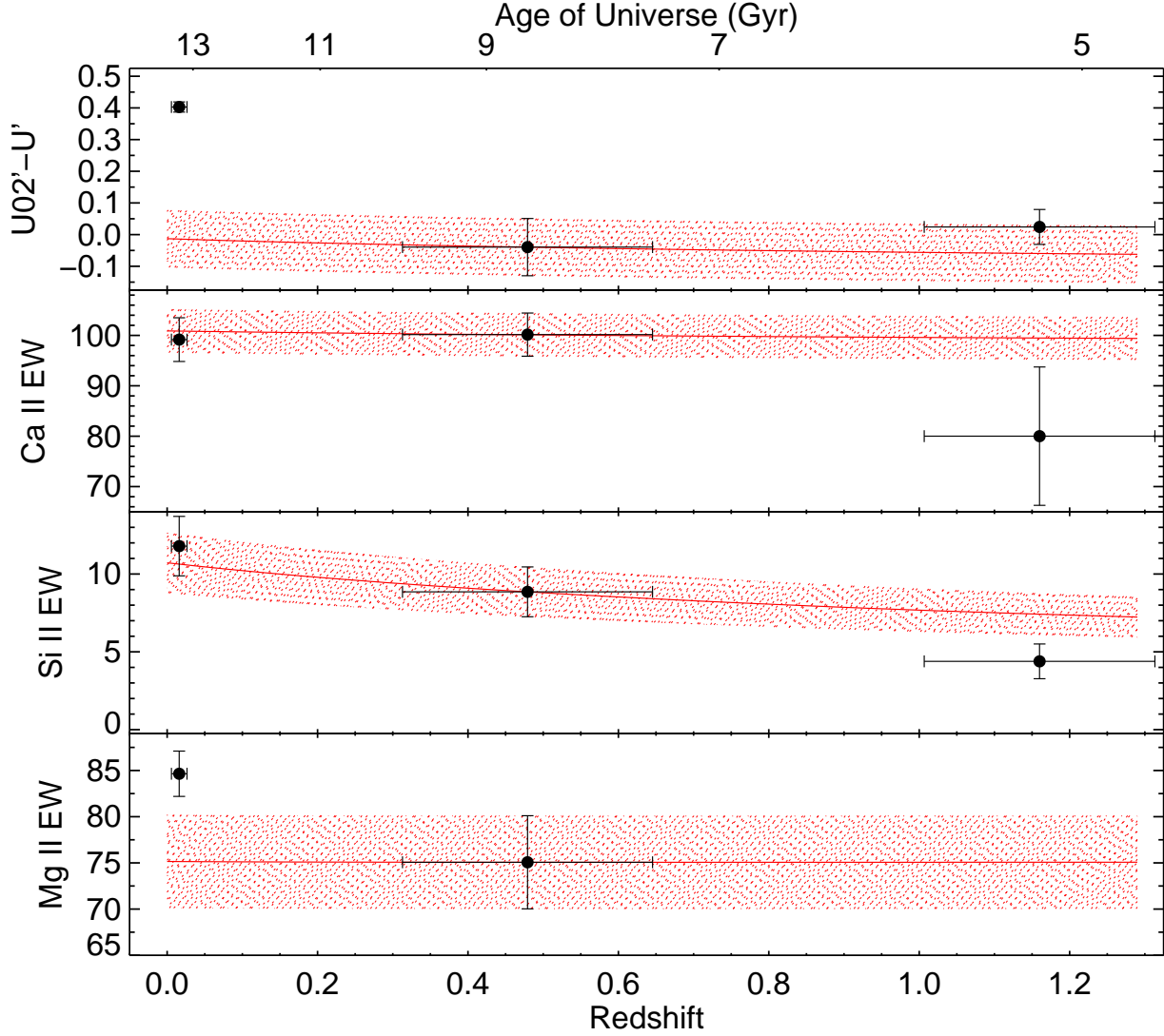


Fig. 3.— The variation with redshift of various features in the three mean spectra. Top panel shows the $U02'-U'$ color measured from the spectra, and the lower three panels show the equivalent width (EW) of the three features Ca II, Si II and Mg II. Redshift errors are the standard deviations of each sample. Overplotted in red is the predicted variation from the observed shift in SN demographics (stretch) with redshift, normalized to the intermediate- z sample; the hashed area shows the uncertainty in this prediction based on the errors in the intermediate- z measurement.

UV scatter from one event to another (E08) may explain such discrepancies. We quantify this “evolution” by measuring a UV-optical color on the mean spectra with two synthetic filters denoted $U02'$ (following Conley et al. 2008) and U' , both marked in Figure 2. Errors are again estimated by analyzing the bootstrapped spectra, and the results are plotted in Figure 3.

4. Discussion

A key question is whether the changes seen in Figures 2 and 3 are a signature of evolution in individual SN Ia properties, or instead a product of changing demographics in the SN population, i.e. the relative increase in SNe Ia from younger progenitors at higher redshift. Are the spectral properties of SNe Ia, at a fixed stretch, evolving with redshift, or is the previously observed redshift drift in the mean stretch causing the observed spectral evolution? To address this, we predict how the various spectral features might be expected to evolve with redshift were a demographic change solely responsible. We use the analysis of Howell et al. (2007), which predicts how the fraction of the two SN Ia components (e.g., ‘A+B’, delayed+prompt, or old+young), and hence the mean SN Ia stretch, changes with redshift. This work is based on the galaxy-type dependent stretch distributions of Sullivan et al. (2006) coupled with a cosmic star formation history and various simple two-component SN Ia rate models (Scannapieco & Bildsten 2005; Mannucci et al. 2006).

We construct a mean spectrum for low and high-stretch SNe Ia based on the sample of E08, defining low-stretch ($s \leq s_0$) and high-stretch ($s > s_0$) sub groups. We use a split point of $s_0 = 1.0$ (e.g. Howell et al. 2007), giving $\bar{s}_{\text{low}} = 0.92$ and $\bar{s}_{\text{high}} = 1.09$. The low-stretch mean is assigned to the “A” (delayed) component, and the high-stretch mean to the “B” (prompt) component. A model mean spectrum for any redshift can then be constructed by combining the two stretch-dependent means in the appropriate ratio of the two components. Predictions for the behavior of the various spectral features can be made by measuring these features on mean spectra constructed at different redshifts, and are over-plotted on Figure 3 (there is some circularity here, as the sample of spectra are also used to make the intermediate- z measurement; however here we are interested in the predicted *change* with redshift rather than the absolute values). The sensitivity of the predictions to the stretch split point is explored varying s_0 by 5%; this has a very minor effect on the results.

The predicted tracks of the model generally match the observations, although the uncertainties remain large. The decrease in Si II EW with redshift is reproduced, though there is evidence that the high- z mean shows an additional deficit in both Si and Ca compared to the lower-redshift spectra. This could also reflect an increase in the fraction of SN1991T-like

events, believed to arise from a younger population, in the $z>1$ sample, where excluding these objects is more difficult due to the lower signal-to-noise of the spectra. The predicted change in UV-optical color fails to match the data, though the robust datasets (E08; R07) show only modest changes consistent with that implied by the change in mean stretch. The main discrepancy occurs with the local data. Such a discontinuous behavior seems unlikely and probably arises from the incomplete sample of local UV spectra, re-emphasizing the need for local, spectroscopically-normal, SNe Ia observed in the UV.

We have shown, for the first time, that the strength of some SN Ia intermediate-mass element spectral features evolve systematically with redshift. However, we hypothesize that this evolution is related to the previously identified shift in SN Ia photometric properties with redshift (Howell et al. 2007), and we show it can be partially modeled using a simple two-component SN Ia rate model and the stretch dependent spectra of E08. After accounting for these expected trends, some small discrepancies in the highest redshift spectra remain, though none at high significance. Thus, we conclude that the observed evolution in SN Ia spectral features can be explained by, and is consistent with, changes in SN Ia demographics, rather than evolution in the properties of individual, photometrically-similar SNe. Controlling for these demographic shifts is the challenge for SN Ia precision cosmology experiments, for example by ensuring that an appropriate k -correction template is used as a function of redshift, and confirming that the empirical relationships used to calibrate SNe Ia in cosmological applications are valid across all environments.

MS and RSE acknowledge support from the Royal Society. PEN acknowledges support from the US Department of Energy Scientific Discovery through Advanced Computing program under contract DE-FG02-06ER06-04. AG acknowledges support by the Benozio Center for Astrophysics, a research grant from Peter and Patricia Gruber Awards, and the William Z. and Eda Bess Novick New Scientists Fund at the Weizmann Institute.

REFERENCES

- Astier, P., et al. 2006, *A&A*, 447, 31
- Branch, D., Lacy, C. H., McCall, M. L., Sutherland, P. G., Uomoto, A., Wheeler, J. C., & Wills, B. J. 1983, *ApJ*, 270, 123
- Bronder, T. J., et al. 2008, *A&A*, 477, 717
- Conley, A., et al. 2008, *ApJ*, 681, 482

- Ellis, R. S., et al. 2008, ApJ, 674, 51
- Filippenko, A. V., et al. 1992, ApJ, 384, L15
- Foley, R. J., et al. 2008a, ApJ, 684, 68
- Foley, R. J., Filippenko, A. V., & Jha, S. W. 2008b, ApJ, 686, 117
- Garavini, G., et al. 2007, A&A, 470, 411
- Guy, J., et al. 2007, A&A, 466, 11
- Höflich, P., Wheeler, J. C., & Thielemann, F. K. 1998, ApJ, 495, 617
- Hamuy, M., Phillips, M. M., Maza, J., Suntzeff, N. B., Schommer, R. A., & Aviles, R. 1995, AJ, 109, 1
- Hamuy, M., Phillips, M. M., Suntzeff, N. B., Schommer, R. A., Maza, J., & Aviles, R. 1996, AJ, 112, 2398
- Hatano, K., Branch, D., Fisher, A., Millard, J., & Baron, E. 1999, ApJS, 121, 233
- Howell, D. A. 2001, ApJ, 554, L193
- Howell, D. A., Sullivan, M., Conley, A., & Carlberg, R. 2007, ApJ, 667, L37
- Jha, S., Riess, A. G., & Kirshner, R. P. 2007, ApJ, 659, 122
- Kirshner, R. P., et al. 1993, ApJ, 415, 589
- Lentz, E. J., Baron, E., Branch, D., Hauschildt, P. H., & Nugent, P. E. 2000, ApJ, 530, 966
- Mannucci, F., Della Valle, M., & Panagia, N. 2006, MNRAS, 370, 773
- Mannucci, F., et al. 2005, A&A, 433, 807
- Matheson, T., et al. 2008, AJ, 135, 1598
- Mazzali, P. A., Röpke, F. K., Benetti, S., & Hillebrandt, W. 2007, Science, 315, 825
- Riess, A. G., et al. 2004, ApJ, 600, L163
- Riess, A. G., et al. 2007, ApJ, 659, 98
- Sarkar, D., Amblard, A., Cooray, A., & Holz, D. E. 2008, ApJ, 684, L13
- Sauer, D. N., et al. 2008, ArXiv e-prints, 803

Scannapieco, E., & Bildsten, L. 2005, ApJ, 629, L85

Sullivan, M., et al. 2006, ApJ, 648, 868